EXPERIMENTAL TEST OF A PROTOTYPE SYSTEM FOR ACTIVE DAMPING OF THE E-P INSTABILITY AT THE LANL PSR*

R. J. Macek#, R. McCrady, S. B. Walbridge, T. Zaugg, LANL, Los Alamos, NM, 87545, USA
C. Deibele, S. Henderson, M. A. Plum, S. Assadi, SNS, Oak Ridge, TN , USA.
J. Byrd, LBNL, Berkeley, CA, USA
S. Y. Lee, Indiana University, Bloomington, IN, USA
M. F. T. Pivi, SLAC, Palo Alto, CA, USA

Abstract

A prototype of an analog, transverse (vertical) feedback system for active damping of the two-stream (e-p) instability has been developed and successfully tested at the Los Alamos Proton Storage Ring (PSR). The system was able to improve the instability threshold (as measured by the RF buncher voltage) by ~30%. This paper describes the feedback system configuration and results of several experimental tests including studies of the factors limiting system performance.

INTRODUCTION

The proton storage ring (PSR) at the Los Alamos National Laboratory (LANL) is an 800 MeV accumulator ring that is used primarily to provide 100 kW of beam for the spallation neutron source at the Los Alamos Neutron Science Center (LANSCE). For this use, PSR delivers 6.25 μC pulses, ~270 ns wide at the base at 20 Hz.

The e-p instability that we proposed to damp has been observed ever since the ring was commissioned in 1985 [1]. It is adequately controlled for the main use by the combination of beam scrubbing and various measures to enhance Landau damping [2], [3] but the increased momentum spread and the non-linearities from most of these measures increase beam losses. Interest in the use of transverse feedback as another means of mitigation is motivated by several factors:

- Transverse feedback would be another tool that has the potential for control without increasing losses.
- For the Spallation Neutron Source (SNS), the interest is that they may need to use feedback to control e-p as the intensity is raised.
- Since the e-p instability for long bunch proton machines is sufficiently different from other instabilities that are controlled by feedback, a proof of principle experiment is a prudent 1st step.
- The present controls at PSR are often not sufficient for the "1st pulse e-p instability" [4] which occurs in a special situation of high peak, smaller emittance, single pulse beams delivered after a long wait time (>15 minutes) with beam off in the ring.

A feedback system for the e-p instability at PSR faces several major challenges besides cost which held off early implementation and which warrant testing before a major investment is made. The instability has a fast growth rate (~50-150 μs e-folding amplitude growth times, 75 μs typical), a broad frequency band (50-300 MHz, depending on intensity) with a central frequency that depends approximately on the space charge density of the beam and is driven by the electron cloud mechanism that is more variable and uncertain than instabilities caused by structural impedances in the accelerator. Thus, the main goal of this collaborative effort was to experimentally investigate the feasibility and effectiveness of feedback damping of the e-p instability with a relatively modest investment in new hardware.

DESCRIPTION OF FEEDBACK SYSTEM

A simplified block diagram of the main components of the prototype system in its final form [5] is shown in Figure 1. An existing short strip line beam position monitor (BPM on the left in Figure 1) was used as the pickup to sense coherent motion from the instability. The vertical difference signal is formed with a suitable hybrid and sent through a variable attenuator to adjust the gain and then through a low pass filter. An RF switch is used for fast gating of the feedback signal. The remainder of the low level RF system (LLRF) consists of a fiber optic delay, a comb filter that can be configured in a number of ways including being bypassed, a low level amplifier and a 180-degree splitter. The split signal is sent to 100 watt RF amplifiers (ENI model 5100L-1431) and then by cable to the downstream end of each plate of the strip line kicker. The upstream ends of the kicker were terminated in 30 dB attenuator loads (50 ohm) whose output could be

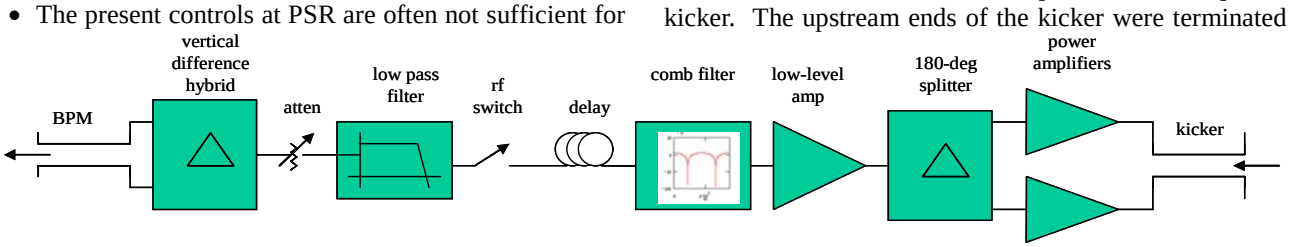

Figure 1. Block diagram of the prototype damping system tested at PSR. Beam direction is right to left.

*Work performed under the auspices of the U.S. DOE,
LANL is supported by U.S. DOE under contract W-7405-ENG-36
#macek@lanl.gov

Contributed to 39th ICFA Advanced Beam Dynamics Workshop on High Intensity High Bightness Hadron Beams 2006 (HB2006), 05/29/2006--6/2/2006, Tsukuba, Japan

Work supported in part by US Department of Energy contract DE-AC02-76SF00515
SLAC, Stanford University, Stanford, CA 94025

monitored or recorded on digital oscilloscopes. Various test points and monitor functions are not shown.

The BPM and the kicker are close to one another in section 4 of the ring with BPM midpoint upstream of the kicker midpoint by 0.76m. For the standard tune the vertical beta functions are calculated in MAD to be 7.5 m and 9.7 m for the BPM and Kicker respectively.

In the absence of the comb filter (or when it is bypassed) and for the nominal vertical betatron tune of Q_y=2.19, a total delay of four turns is needed for the signal between the BPM and the feedback waveform applied to the kicker to produce an odd number times 90 degrees of betatron phase advance for optimal damping. The comb filter section (added later in order to suppress revolution harmonics) was of a modular design using fiber optic delays and could be configured as one or two comb filters in series and each filter could be set independently with one or two turns of delay.

Standard transverse feedback theory assumes that the angular kick delivered by the kicker is proportional to the beam position at the pickup [6]. However, the vertical difference signal from the short strip line BPM is not proportional to the beam centroid position but is approximately the time derivative of the position multiplied by intensity for the frequencies of interest. It is nevertheless a useful signal for feedback if the bandwidth of the coherent motion is not too broad (< ± 15%) in which case integration is approximately achieved by a 90 degree phase shift at the central frequency.

For a strip line kicker we used an existing device that was designed as a BPM. A cross-sectional sketch is shown in Figure 2 (left). The curved plates are at a radius of 51 mm inside a beam pipe with a 76 mm radius. Each curved plate subtends an angle of ~114 degrees. The physical length of the curve plates is 0.37 m. Numerical calculations give a value of 48 ohm for the impedance of the strip lines. Estimates of the effective transverse shunt impedance (which includes the transit time effect) of this stripline were made using the approximate analytical formula for the effective shunt impedance, $R_\perp$, (equation 1 below) which assumes a plane wave propagating between parallel plates [7]. Note that the deflection from the kicker will be proportional to the square root of the product of applied power and the shunt impedance.

$$R_\perp = 2Z_L\left(\frac{2g_\perp c\beta}{\omega d}\right)^2 \sin^2\left(\frac{\omega L(1+\beta)}{2c\beta}\right) \qquad (1)$$

In this formula, Z_L is the termination load impedance, L, the length of the stripline plate, d, the plate separation, ω, the angular frequency, β, the beam velocity divided by c, the velocity of light and $g_\perp$, a geometry factor of order unity. The shunt impedance calculated using equation (1) is plotted in Figure 2 (left).

The frequency response of the LLRF, the comb filters, the final amplifiers and the kicker have been measured with a network analyzer for signals that do not saturate the components. These show bandwidths that are comparable to or better than those of the kicker shunt impedance shown in Figure 2 right.

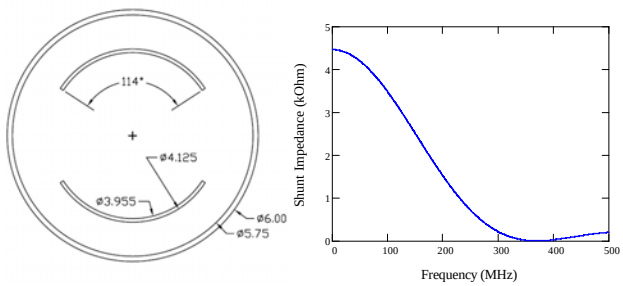

Figure 2. (Left) Cross-section of the kicker; dimensions are inches and degrees. (Right) Shunt impedance vs. frequency for the PSR kicker for L =0.37m.

DAMPING TESTS

Measures of feedback effectiveness

The earliest and simplest evidence of useful damping of e-p was demonstrated by accumulating a 3 μC beam intensity (with feedback off) and storing for 500 μs after the end of accumulation then lowering the RF buncher voltage in the ring until the instability threshold was reached. At this point there was significant and growing coherent transverse motion of the beam centroid (red trace in Figure 3) accompanied by significant beam loss. When the feedback was turned on, the unstable motion disappeared (blue trace in Figure 3).

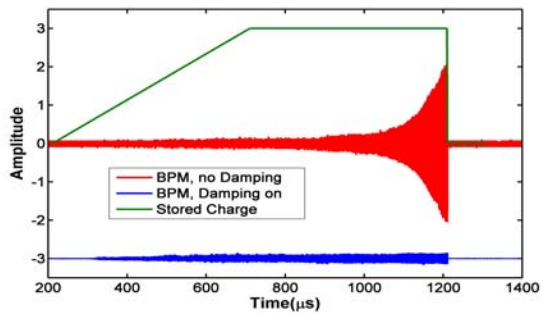

Figure 3. Vertical difference signal from the BPM at instability threshold with feed back off (red) compared to the BPM signal when feedback was on (blue). The green trace shows the circulating beam current in the ring.

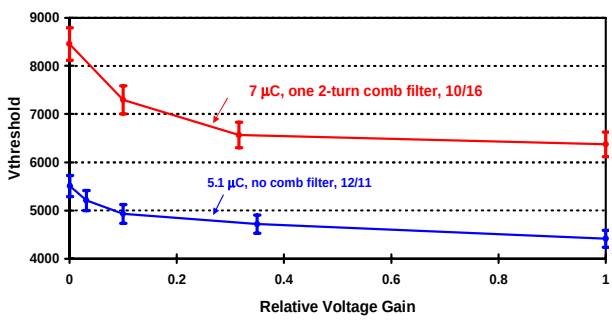

Figure 4. Instability threshold (RF buncher voltage) as a function of relative gain of the feed back system for two different situations indicated by the curve labels.

Our principal quantitative measure of effectiveness for the damping system is the change in instability threshold with feedback on compared with the value when feedback

is off. Since it is easier to change the buncher voltage than the beam current, we use variation of the buncher voltage to find the threshold. The two variables are essentially equivalent as demonstrated by the well-established linear relationship between the two at PSR. A plot of threshold voltage as a function of the relative feedback system voltage gain is shown in Figure 4. These curves show a maximum improvement in instability threshold of 25% between feedback off and feedback on at the highest gain. We were not able to significantly improve upon this result and devoted much effort to identification and analysis of the limiting factors.

Grow-damp experiments

Gating the RF switch in the LLRF with a suitable wave form enabled us to perform grow-damp experiments which offer the capability to measure instability growth rates during the growth phase and the damping rates with feedback on in the damp phase. These experiments were performed with the buncher voltage set to be half way between the threshold for feedback on and feedback off. Signals from a damp-grow-damp experiment using a 7 μC/pulse beam on 10/16/05 are shown in Figure 5.

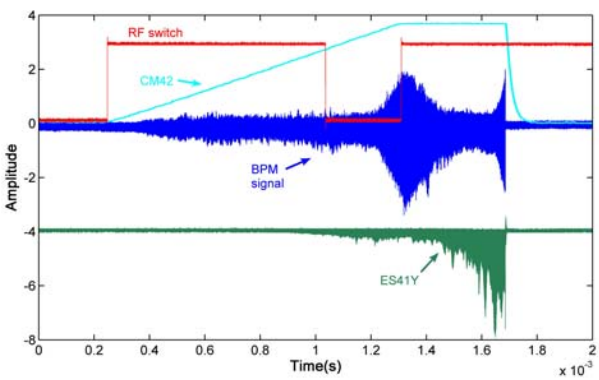

Figure 5. Plot of signals from one beam pulse in a grow-damp-grow experiment. Shown are the BPM signal (blue) filtered with a 300 MHz digital filter, the rf switch signal (red), the stored beam current monitor, CM42.

The instability in Figure 5 started to grow after feedback was turned off and then damped when the feedback was gated on again at the end of accumulation. The second period of growth that shows up at the end just before extraction will be discussed later. While there are several ways to define and measure growth rates, we have chosen to calculate the power spectral density (PSD) and sum over a band of modes in order to obtain a single parameter. The PSD is calculated from the square of the fft amplitude using non-overlapping rectangular time windows and plotted as a function of time and mode # ($\omega/\omega_{rev} + Q_y$) in Figure 6.

The log of the PSD sum is plotted as a function of time in Figure 7 and the slopes of growth and damping regions were measured. The exponential growth and damping rates (e-folding times)$^{-1}$ for power obtained from the plot of Fig. 10 are 20600, -14400, 31900 in units of s^{-1} for the 1st growth region, the damping region and the 2nd growth region respectively. The power damping rate for the feedback system would be 20600+14400=35000. If the damping system is still operating in the linear region, then the appearance of the second growth region implies that the underlying instability growth rate exceeds the damping rate and we would infer a growth rate of 35000+31900=66900 for the instability in the second region. This is a factor of ~3 higher than for the first growth region (no feedback) and ***twice the power damping rate*** for the feedback system.

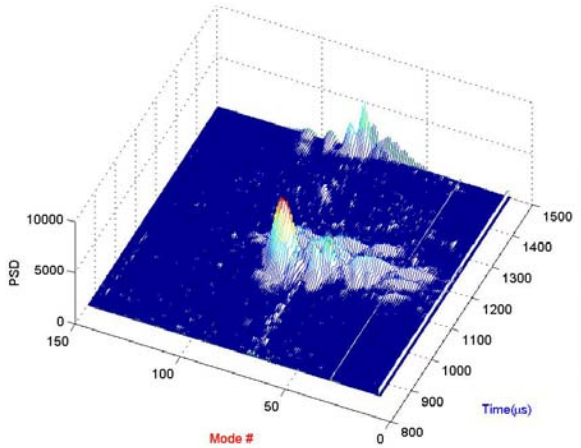

Figure 6. PSD spectrogram of BPM signal of Figure 6.

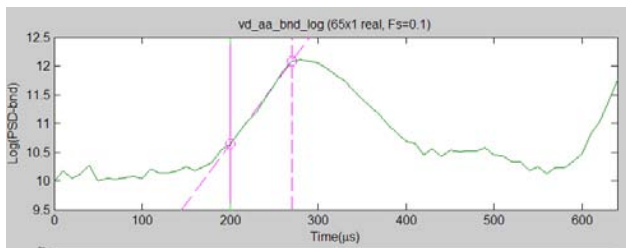

Figure 7. Plot of the log of the PSD summed over modes 25-125; e-folding growth time is 49 μs for the power.

The second growth phase is a puzzle. It is not likely due to saturation of the feedback system since the power applied to the kicker was not at its maximum for the second growth phase as shown in the plot of the voltage at the upstream end of the kicker striplines (Figure 8).

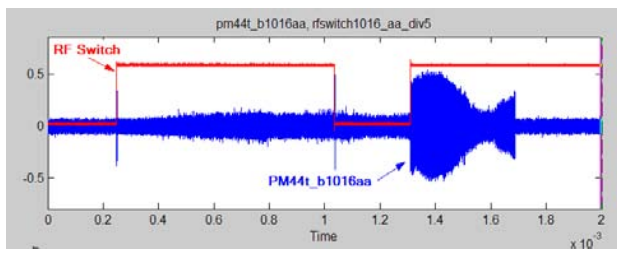

Figure 8. Plot of the voltage (50dB attn.) at the upstream end of the kicker striplines (blue trace, PM44t_b1016aa).

One clue to a possible explanation of the puzzle may be the increase in multipactor electrons during the store as shown in the bottom plot in Figure 5 (green trace) which is a signal from an electron detector (ES41Y) located in a drift space. It detects the electrons striking the wall and shows a factor of 5 or more increase over the 400 μs storage time. While such evidence is suggestive it is not

conclusive proof that more electrons survived the gap to be captured by the next beam pulse since previous studies in 2001 have shown that electrons surviving a clean gap saturate at these intensities. There has been continual beam scrubbing since then so the intensity for saturation might have changed to a higher value.

LIMITING FACTORS

Beam in the gap

If there is some beam-in-the-gap (BIG) more of the multipacting electrons will survive the gap and be captured by the next pulse. Other studies in 2001, 2002, and 2006 where controlled amounts of beam were introduced in the gap, demonstrated a linear relationship between electrons surviving the gap and the amount of BIG such that adding a certain amount of BIG will increase the number of electrons surviving the gap by an amount that will neutralize the BIG.

Figure 9 shows that a significant amount of BIG developed during the 400 μs store time for the damp-grow-damp example discussed earlier. There is little BIG at the end of injection when the feedback was turned on (blue trace Figure 9). By the start of the second instability growth phase (red trace Figure 9) there is evidence of beam leakage into the gap consistent with a level of ~2% of the peak current. This level would be roughly consistent with a factor of about 3 increase in the growth rate, assuming that it depends linearly on neutralization of the beam by the electrons surviving the gap.

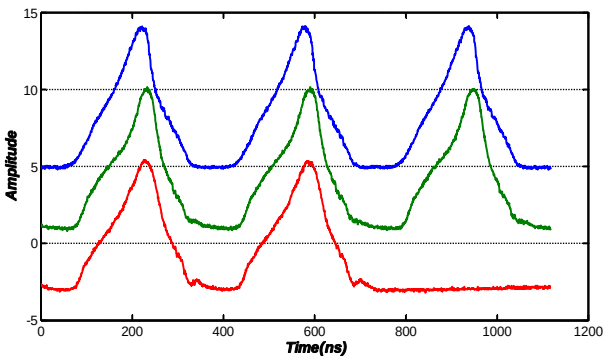

Figure 9. Turn-by-turn expansion of the signal from a wall current monitor (WC41) at three different times in the beam pulse; at end of injection (blue), near start of second growth period (green) and at extraction (red).

The lower buncher voltage made possible with feed back lowers the rf bucket height and can cause beam leakage into the gap, which suggests a possible explanation for the limited improvement in instability threshold with feedback. This was certainly exacerbated by poor control of the energy of the beam from the linac as a result of problems with some of the linac power amplifiers during the 2005 run cycle. For comparison, the wall current signal (Figure 9) for an unstable 8.3 μC beam in 2002 showed no beam in the gap even at extraction.

Other features of note in Figure 8 relate to the changes in the shape of the longitudinal profile of the beam during the store time. During the typical PSR accumulation time there are only 1-2 synchrotron periods (~ 500 μs) and therefore the beam is not, in general, particularly well matched in longitudinal phase space. Thus, the longitudinal profile can change during the store time as the beam rotates in longitudinal phase space. In addition, the bunch width is a large fraction of the bucket width which produces a slower synchrotron frequency for the protons injected near the ends of the bunch. The changes in pulse shape during the store can also have a strong impact on the electron cloud generation by trailing edge multipactor and may explain the strong increase in the electron detector signal during the store as shown in Figure 6.

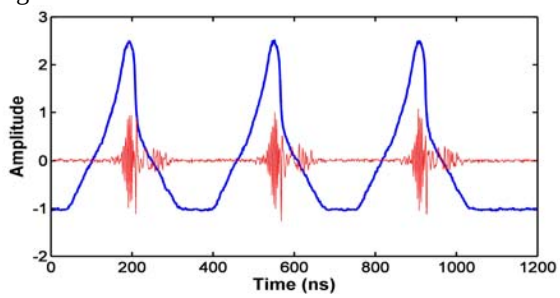

Figure 10. Wall current signal for an 8.3 μC unstable beam in 2002 shows no beam in gap at extraction. The BPM signal of unstable motion is the red trace in proper time relationship to the beam pulse.

Feedback power limitations

From an electrical engineering viewpoint the prototype system performed as intended. The low loss fiber optic delay lines were essential to obtaining the 4 turn delay. The comb filters had excellent electrical characteristics with deep notches at the revolution harmonics. The main system concerns from the beginning were feedback gain/power and bandwidth. Output power of 100 watts for each kicker plate was estimated to be adequate for amplitude growth times of ~75 μs typically encountered for 5-6 μC beams and centroid motion amplitude of 1mm at full feedback power. From the damping rate measured in grow-damp experiments we estimate that the feedback system could handle growth times down to 50-60 μs.

The measured bandwidth of 10 to 300 MHz of the feedback amplifier system would cover most of the observed frequency content for the instability at intensities up to ~6 μC/pulse for the standard beam emittance encountered in routine operations for the LANSCE spallation neutron source. In our beam tests of the prototype system we saw no clear evidence that system bandwidth was limiting performance such as unstable motion outside the bandwidth. An exception might be the smaller emittance, high space charge beams which await more detailed analysis. The first pulse instability typically has higher frequencies but we did not have the opportunity to investigate the effectiveness of feedback in a controlled way for this situation.

The fast growth rates encountered on some pulses when the buncher voltage was lowered to the instability

threshold with feedback on (e.g. the second growth phase in Figures 5-7) were somewhat unexpected. Our studies described in earlier sections suggest that these were caused by beam leakage into the gap between bunches such that more electrons survive the gap to be captured by the next beam pulse and drive the instability more vigorously. The need to know the shortest growth time to be damped and the factors affecting it prompted us to under take a systematic examination of earlier data on growth times at instability threshold for 8.3, 5.0 and 3.0 μC beams which had no BIG [8]. This study showed considerable variability from pulse to pulse (50-200 μs) and no significant dependence on intensity. The 50 μs amplitude growth time is at the limit of the prototype feedback system capabilities and allows no headroom for faster growth from BIG.

The special situations that give rise to the 1st pulse instability typically use the maximum voltage available from the RF buncher. We did have feedback on for one such run but it was not enough to stabilize the beam. Amplitude growth times as low as 8.8 μs have been observed for the 1st pulse instability, which would require much more feedback power (and/or more kickers) to control than available with the prototype system.

Role of the horizontal instability

In one test (6/30/05, 5.1 μC beam) with feedback on, we did observe the appearance of the instability in the horizontal plane at threshold and it started before the vertical instability appeared. In this experiment the feedback was on and the RF buncher voltage lowered to the threshold of the instability (30% lower voltage) and unstable coherent motion first appeared in the horizontal plane. The BPM vertical difference (blue trace) and horizontal difference (red trace) signals are shown in Figure 11. A comparison of the two shows that the horizontal motion starts earlier.

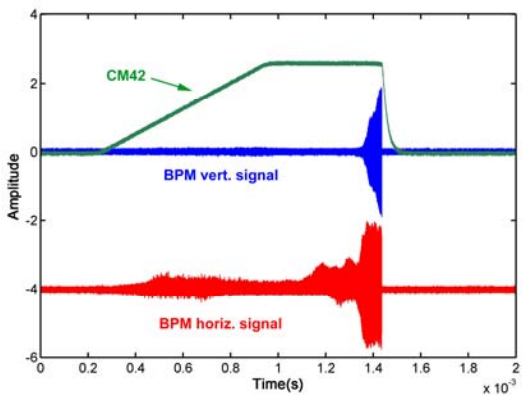

Figure 11. Vertical difference signal (blue) from the BPM and horizontal difference signal (red) for 6/30/05 test. A signal from the beam current monitor (green) in the ring is also shown to indicate the accumulation and store times.

It is not surprising that the instability eventually shows up in the horizontal when the vertical is damped by feedback. In the simple coasting beam theory with Landau damping the threshold is proportional to betatron tune, hence, in the absence of feedback and all other things being equal, the vertical is more unstable by virtue of the smaller Q_y=2.19 compared to Q_x=3.19. However, with feed back stabilizing the vertical motion the horizontal plane will become unstable as the buncher voltage is lowered and the Landau damping is insufficient to overcome the horizontal e-p growth rate. In this simple model one expects the horizontal to become unstable at a buncher voltage that is ~30-50% lower, which is consistent with observations.

CONCLUSIONS

The prototype feedback system described here and tested at PSR was able to improve the e-p instability threshold by ~30%. Further improvement appeared to be limited mainly by three factors: 1) Beam leakage into the gap between bunches brought on by the lower RF buncher voltage and abnormal energy variations (energy droop during the macropulse) of the beam injected into the ring. 2) Higher than expected variations in growth rates produce maximum growth rates higher than expected and therefore higher feedback power requirements and/or more kickers. 3) Onset of the instability in the horizontal plane which did not have feedback. The appearance of the instability in the horizontal plane was anticipated in the analytical coasting model for e-p. For maximum effectiveness both planes should have feedback.

ACKNOWLEDGMENTS

We gratefully acknowledge the dedicated beam time and other support provide by LANSCE division at LANL as well as numerous helpful discussions with Doug Gilpatrick, John Powers and Larry Rybarcyk. The authors would also like to acknowledge the splendid efforts of the operating crews at LANSCE who made every effort to meet the beam requirements for these studies.

REFERENCES

[1] D. Neuffer et al, Nuclear Instrumentation and Methods in Physics Research A321 (1992), 1-12.
[2] R. J. Macek et al, Proceedings PAC 2001, Vol. 1, p 688-692.
[3] R. J. Macek et al, Proceedings of 31st ICFA Beam Dynamics Workshop on Electron Cloud Effects 'ECLOUD04', April 19-23, 2004, Napa, CA, CERN Report 2005-001, p 63-75.
[4] R. J. Macek, et al, THAW04, HB2006 workshop.
[5] C. Deibele et al, THPCH130, EPAC06 (2006).
[6] J. Rogers, Handbook of Accelerator Physics and Engineering, eds. Chao and Tigner, p 490.
[7] S. Henderson, http://www.sns.gov/APGroup/instability/instability.html. (11/22/2004).
[8] R. J. Macek et al, LANL report, LA-UR-06-2084, (3/16/2006).